Acta Crystallographica Section D
Biological Crystallography
ISSN 0907-4449

Crystallization and preliminary X-ray diffraction analysis of a novel pectate lyase from *Azospirillum irakense*

Hector Novoa de Armas,[a] Anja Rabijns,[a] Christel Verboven,[a] Jos Desair,[b] Ann Vande Broek,[b] Jozef Vanderleyden[b] and Camiel De Ranter[a]*

[a]Laboratorium voor Analytische Chemie en Medicinale Fysicochemie, Faculteit Farmaceutische Wetenschappen, K. U. Leuven, E. van Evenstraat 4, B-3000 Leuven, Belgium, and [b]Centrum voor Microbiële en Plantengenetica, K. U. Leuven, Kasteelpark Arenberg 20, B-3001 Heverlee, Belgium

Correspondence e-mail: camiel.deranter@farm.kuleuven.ac.be

Received 3 August 2001
Accepted 24 October 2001

The *PelA* gene from the N_2-fixing plant-associated bacterium *Azospirillum irakense* encodes a pectate lyase. Analysis of the corresponding amino-acid sequence revealed no homology to other bacterial, plant and fungal pectinases of known published structure, resulting in the classification of the enzyme in a new pectate lyase family. The *A. irakense* PelA has been crystallized using the hanging-drop vapour-diffusion method at 277 K. The crystals are hexagonal, with unit-cell parameters $a = b = 85.55$, $c = 230.13$ Å, $\gamma = 120^\circ$, and belong to space group $P6_522$ or $P6_122$, having one molecule per asymmetric unit. Diffraction data to a resolution of 1.97 Å were collected at synchrotron facilities, as well as a three-wavelength MAD data set from an Hg-derivative crystal to a resolution of 2.6 Å.

1. Introduction

Disease-causing bacteria infect and spoil stored fruits and vegetables. During 'soft-rot' spoilage, pectin, a major structural polysaccharide in the plant cell wall, is enzymatically degraded, leading to the deterioration of fruit and vegetable tissue. Pectin is depolymerized by a combination of enzymatic activities of a group of carbohydrate-active enzymes: pectin methyl esterase, pectin acetyl esterase, pectin lyase, pectate lyase and polygalacturonase. Lyases can cleave polygalacturonate (PGA) glycosidic bonds in an exo or endo fashion *via* β-elimination, producing oligomers with 4,5-unsaturated residues at the non-reducing end. In contrast, polygalacturonase hydrolyzes the polymer, yielding saturated products.

Pectinolytic enzymes are usually associated with virulence of a number of phytopathogenic bacteria. The genetics of pectinase biosynthesis in these phytopathogens, especially in the soft-rotting *Erwinia* species *E. carotovora* and *E. chrysanthemi*, has been extensively studied in the past decade. Both species were found to produce a set of pectin-depolymerizing enzymes such as pectate lyases, polygalacturonases, pectin methyl esterases and a pectin acetyl esterase (Barras *et al.*, 1994; Hugouvieux-Cotte-Pattat *et al.*, 1996; Pissavin *et al.*, 1996; Shevchik *et al.*, 1997; Shevchik & Hugouvieux-Cotte-Pattat, 1997). Of these, the pectate lyases are the major pectinases and play a key role in the development of soft-rot disease. In addition to in phytopathogens, pectin depolymerization has also been reported in non-pathogenic plant-associated bacteria such as the N_2-fixing endosymbiont *Rhizobium* (Mateos *et al.*, 1992; Hubbell *et al.*, 1978) and the N_2-fixing soil bacterium *A. irakense* (Bekri *et al.*, 1999). Isolates of *A. irakense* were obtained from surface-sterilized field-grown rice roots (Khammas *et al.*, 1989), indicating their capacity to penetrate plant roots and suggesting the involvement of plant cell-wall degrading enzymes (*i.e.* pectinases) in this infection process. A gene encoding a pectate lyase (termed PelA) from *A. irakense* was isolated by heterologous expression of the gene in *Escherichia coli* (Bekri *et al.*, 1999). The initial analysis of the corresponding amino-acid sequence revealed no homology to other bacterial, plant and fungal pectinases, leading to the classification of the enzyme in a new pectate lyase family (family 10).

Currently, there are a number of pectate lyases (PelE and PelC from *E. chrysanthemi*, Pel15 from *Bacillus* sp. strain KSM-P15 and PEL from *B. subtilis* strain S1103) of which the crystal structures have been reported in crystallographic databases (Jenkins *et al.*, 1998; Akita *et al.*, 2000; Pickersgill *et al.*, 1994), but the structure of a non-phytopathogenic pectate lyase has yet to be published. Since *A. irakense* has never been reported to be pathogenic to plants, the structure of *A. irakense* PelA would be particularly interesting to identify potential differences with phytopathogenic pectate lyases. The mature PelA protein is a single-

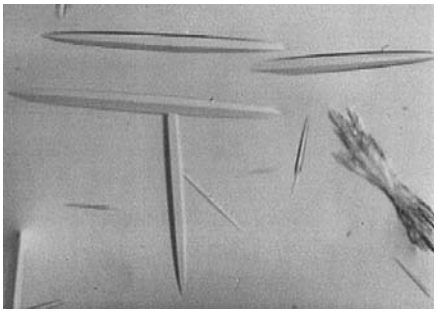

Figure 1
Hexagonal crystals of *A. irakense* PelA.

domain enzyme that contains 408 amino acids and has a calculated molecular mass of 44.5 kDa.

Based on sequence homology, pectate lyases have been classified into ten distinct families. Recently, new members of family 10, originally defined by *A. irakense* PelA, were reported: Pel-15E from *Bacillus* sp. strain KSM-P15 (Sawada *et al.*, 2000) and Pel10A from *Pseudomonas cellulosa* (Brown *et al.*, 2001). Pel-15E possesses some regions that are homologous to PelA with an overall amino-acid identity of 39.8%. The 35.8 kDa C-terminal module of Pel10A was shown to have 33.5 and 36.6% amino-acid identities with PelA and Pel-15E, respectively. Very recently, the catalytic module of Pel10A (Pel10Acm, residues 325–644) has been crystallized (Charnock *et al.*, 2001). The optimum activity of PelA was seen at pH 9, which is comparable to the value of pH 10 for the optimum activity of Pel10Acm from *P. cellulosa* and pH 10.5 for Pel-15E from *Bacillus sp*. This is a remarkable feature of pectate lyases: their optimum pH always falls in the range pH 8.5–10.5 independently of whether the microorganism that produces the pectate lyase is neutrophilic or alkaliphilic.

The crystal structure of these enzymes will provide detailed three-dimensional information on this most recently discovered family of lyases, leading to the identification of the key residues in the substrate binding and the lyase catalytic mechanism. Here, we report the purification, crystallization and preliminary X-ray crystallographic characterization of the *A. irakense* PelA protein.

2. Experimental

2.1. Protein expression and purification

E. coli DH5α(pFAJ0612) (Bekri *et al.*, 1999) was grown at 310 K in LB broth to the stationary growth phase. The culture was centrifuged at 6000*g* for 20 min and the pellet, after freezing at 253 K, was resuspended to a final concentration of 20%(*w*/*v*) in 50 m*M* sodium acetate buffer pH 5 containing 400 U DNAseI per millilitre. Cells in this suspension were lysed in FastRNA tubes (BIO101) with a FastPrep FP120 device (Savant). The pH of the lysate was adjusted to pH 5 with acetic acid and the lysate was subsequently clarified by centrifugation and ultrafiltration. Clarified lysate was then loaded onto an SP Sepharose HP XK16/10 column (Amersham Pharmacia Biotech) and, after rinsing with 50 m*M* sodium acetate buffer pH 5, eluted in 60 min with a linear gradient of 0–300 m*M* NaCl at a flow rate of 1 ml min^{-1}. PelA activity in the different fractions was assayed by photometric monitoring upon incubation with polygalacturonic acid as described by Bekri *et al.* (1999). PelA active fractions were pooled and HIC buffer [1.7 *M* $(NH_4)_2SO_4$, 20 m*M* Tris pH 7.4] was added to a final concentration of 1 *M* $(NH_4)_2SO_4$. This sample was loaded onto a phenyl Sepharose HP XK16/10 column (Amersham Pharmacia Biotech) and, after rinsing with 1 *M* $(NH_4)_2SO_4$, 20 m*M* Tris–HCl pH 7.4, eluted in 40 min with a linear gradient of 0–20 m*M* Tris–HCl pH 7.4 at a flow rate of 1 ml min^{-1}. Fractions exhibiting Pel activity were concentrated using Vivaspin6 5000 MWCO concentrators (Vivascience) according to the manufacturer's instructions. The final isolate was then purified and desalted by gel filtration through a Superdex200pg XK16/60 column (Amersham Pharmacia Biotech), using 50 m*M* NaCl, 20 m*M* Tris–HCl pH 7.2 at a flow rate of 1 ml min^{-1}.

2.2. Dynamic light-scattering study

The dynamic light-scattering (DLS) of the PelA sample was performed on a Model DynaPro-MS TC200/12 instrument from Protein Solutions (Charlottesville, Virginia). The data were measured at room temperature with 5 mg ml^{-1} of protein in a buffer containing 75 m*M* sodium chloride. The sample was filtered through a 0.02 µm pore-size Anotop-10 inorganic membrane filter (Whatman) just prior to DLS measurement and used to fill the cell. A set of 65 measurements of 5 s each was recorded.

2.3. Crystallization

Prior to crystallization, the protein solution was concentrated to approximately 10 mg ml^{-1} by ultrafiltration using a Microcon concentrator (Amicon) with a 3 kDa cutoff. The initial crystallization conditions were established using sparse-matrix sampling (Jancarik & Kim, 1991) with hanging-drop vapour-diffusion geometry at 277 K using Crystal Screens I and II (Hampton Research). A hanging drop was prepared by mixing equal volumes (2 µl each) of protein and the reservoir solution. Each hanging drop was placed over 700 µl of reservoir solution.

2.4. X-ray diffraction experiment

Prior to flash-freezing, crystals were soaked for 30 min in a cryoprotectant solution consisting of the crystallization solution plus 25% glycerol. The crystals were mounted in cryoloops and then plunged into liquid nitrogen. The cryoloops were placed on a goniometer head and maintained at 100 K during diffraction data collection. Diffraction data for the native and heavy-atom treated crystals were collected using synchrotron-radiation sources at EMBL-DESY (Hamburg) and Elettra (Trieste), respectively.

Table 1
Synchrotron data-collection statistics.

Values in parentheses refer to the highest resolution shell (2.01–1.97 Å).

Crystal data for type III native PelA crystals (DESY, 2000).

Crystal system	Hexagonal
Space group	$P6_522$
Unit-cell parameters (Å, °)	$a = b = 85.55$, $c = 230.13$, $\gamma = 120$
X-ray source	BW7B DESY
Resolution range (Å)	30–1.97 (2.01–1.97)
Total No. of reflections	292835
No. unique reflections	36238 (1764)
Completeness (%)	100 (99.9)
Multiplicity	8.1 (6.3)
$R_{\rm merge}$†	5.3 (35.0)
$\langle I/\sigma(I)\rangle$	13.1 (1.5)

Heavy-atom statistics for MAD phasing of mercury derivative.

λ_1 (Å)	0.918407
λ_2 (Å)	0.991880 (reference)
λ_3 (Å)	1.010719
Resolution (Å)	2.65
Completeness (%)	$\lambda_1 = 97.3$ (98.3), $\lambda_2 = 100$ (99.9), $\lambda_3 = 98.1$ (98.1)
R for dispersive differences	$\lambda_3 - \lambda_1 = 0.070$, $\lambda_3 - \lambda_2 = 0.06$
R for anomalous differences	$\lambda_1 = 0.033$, $\lambda_2 = 0.039$, $\lambda_3 = 0.055$
Overall figure of merit for MAD phasing (before density modification)	0.44 (0.5–2.6 Å)

† $R_{\rm merge} = 100\sum_h \sum_i(|F^2_{hi} - \langle F^2_{hi}\rangle|)/\sum_h \sum_i F^2_{hi}$, where F^2_{hi} is the square of the ith intensity measurement of reflection h and $\langle F^2_{hi}\rangle$ is the mean-squared intensity of the reflection.

The diffraction data of the native crystals were collected using a MAR 345 imaging-plate detector. The three-wavelength MAD data set from the heavy-atom (Hg) soaked crystal was collected using a MAR CCD 165 mm detector. The *DENZO* and *SCALEPACK* packages (Otwinowski & Minor, 1997) were used for the determination of the unit-cell parameters, data indexing, reduction and scaling. Patterson maps were initially generated with the routine *MAPVIEW* from the *PHASES* program (Furey & Swaminathan, 1990). The program *SHARP* (de La Fortelle & Bricogne, 1997) was used to confirm and refine heavy-atom sites as well as to find possible additional sites.

3. Results and discussion

The purified protein sample ran as a single band on SDS–PAGE, with an apparent mobility equivalent to a molecular mass of 44 kDa. The size-distribution function obtained by dynamic light-scattering measurements shows a narrow profile with a mean radius of 2.99 nm, which corresponds to a theoretical molecular-weight value of 46.5 kDa, with a polydispersity of 23.1%. This means that the protein exists as a monomer in solution. Two different types of crystals were first obtained from 5% isopropanol and 2.0 *M* ammonium sulfate (type I) and 20% isopropanol, 20% PEG 4000 and 0.1 *M* citrate pH 5.6 (type II). By changing the pH, the concentrations of precipitants, the temperature and the ratio of protein to reservoir solution in the hanging drop, the initial crystallization conditions were further refined. Both crystal types usually grow in one week. The type I crystals, having a diamond shape, were further improved in size by either adding 0.1 *M* magnesium chloride or sodium chloride to the crystallization condition; however, they did not diffract.

The type II crystals were improved by adding 0.2 *M* ammonium sulfate to the original crystallization conditions. A suitable crystal for X-ray diffraction was found after about four months. This crystal was tetragonal, with space group *P*422 and unit-cell parameters $a = b = 94.37$, $c = 103.98$ Å. An 88% complete native data set ($R_{\rm sym} = 15.4\%$) was collected to 3.5 Å at the X11 beamline of the DESY synchrotron, Hamburg. However, these crystals took a long time to grow and the resolution was poor. Further improvement of this crystallization condition to 15% isopropanol, 0.1 *M* imidazole pH 7.8 and a 2:1 ratio of protein to reservoir solution in the hanging drop gave rod-shaped (type III) crystals (Fig. 1) with approximate dimensions of 0.6 × 0.1 × 0.1 mm. These crystals are hexagonal, with unit-cell parameters $a = b = 85.55$, $c = 230.13$ Å, $\gamma = 120^\circ$. They diffract to 1.9 Å and a complete data set to 1.97 Å was collected at DESY beamline BW7B (Hamburg). The statistics for this data set are shown in Table 1. From the symmetry of the intensity-weighted reciprocal lattice and systematically absent reflections (the absence of 00*l* reflections for $l \neq 6n$), the possible space groups were $P6_122$ and $P6_522$. Using the Matthews formula (Matthews, 1968), one molecule in the asymmetric unit and a water content of 56% were predicted. Fig. 2 shows a 1° oscillation image of a native crystal. Heavy-atom derivative screening identified a mercury isomorphous derivative when type III native PelA crystals were soaked in 0.5 m*M* ethylmercury phosphate for 24 h; the heavy-atom salt solution was prepared with 0.2 *M* lithium sulfate instead of 0.2 *M* ammonium sulfate. From the data set collected from such an Hg-derivative crystal, it was possible to locate one Hg site in the anomalous Patterson map (Fig. 3) and to refine this site (isomorphous and anomalous phasing powers after refinement were 2.53 and 1.19, respectively, to 2.6 Å resolution). Structure determination using the MAD method (Hendrickson, 1991) is presently under way on a three-wavelength data set collected at the Elettra Synchrotron, Trieste. The statistics for this MAD data set are also shown in Table 1.

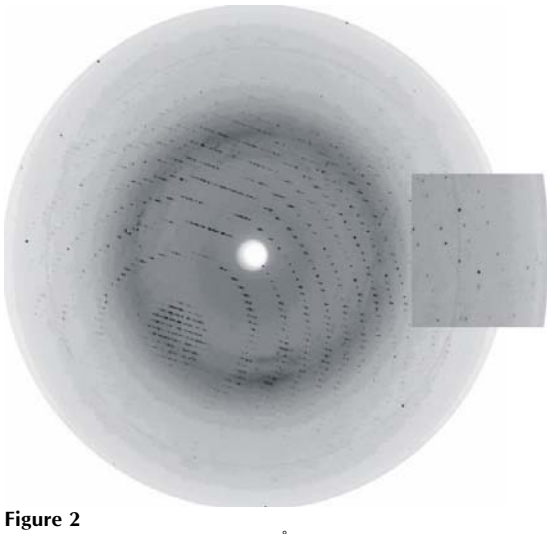

Figure 2
Diffraction pattern from the 1.97 Å native PelA data set. The edge of the plate corresponds to 1.97 Å resolution.

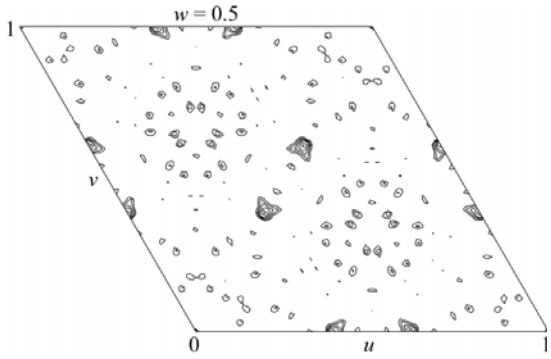

Figure 3
Anomalous Patterson map for the ethylmercury phosphate derivative of PelA.

HNDA would like to thank the K. U. Leuven, Belgium for an IRO scholarship. AR is a Postdoctoral Research Fellow of the Fund for Scientific Research-Flanders (Belgium). CV is a Postdoctoral Research Fellow of the K. U. Leuven Research Fund (OT/98/38). Walter Jottier is acknowledged for technical assistance during in-house preliminary data collection. We acknowledge the support of the protein crystallography project team at the EMBL BW7B beamline at the DORIS storage ring, DESY, Hamburg and the staff of beamline 5.2R, Elettra, Trieste. The European Union is acknowledged for supporting the work at EMBL Hamburg (HCMP to Large Installations Projects, contract No. CHGE-CT93-0040) and at Sinchrotrone Trieste (Human Potential Programme Transnational Access to Major Research Infrastructures, contract No. HPRI-CT-1999-00033).

References

Akita, M., Suzuki, A., Kobayashi, T., Ito, S. & Yamane, T. (2000). *Acta Cryst.* D**56**, 749–750.
Barras, F., van Gijsegem, F. & Chatterjee, K. A. (1994). *Annu. Rev. Phytopathol.* **32**, 201–234.
Bekri, M. A., Desair, J., Keijers, V., Proost, P., Searle-van Leeuwen, M., Vanderleyden, J. & VandeBroeck, A. (1999). *J. Bacteriol.* **181**, 2440–2447.
Brown, I. E., Mallen, M. H., Charnock, S. J., Davies, G. J. & Black, G. W. (2001). *Biochem. J.* **355**, 155–165.
Charnock, S. J., Brown, I. E., Turkenburg, J. P., Black, G. W. & Davies, G. J. (2001). *Acta Cryst.* D**57**, 1141–1143.
Furey, W. & Swaminathan, S. (1990). Am. Crystallogr. Assoc. Meet. Abstr., p.73. Abstract PA33.
Hendrickson, W. A. (1991). *Science*, **254**, 51–58.

Hubbell, D. H., Morales, V. H. & Umali-García, M. (1978). *Appl. Environ. Microbiol.* **35**, 210–213.
Hugouvieux-Cotte-Pattat, N., Condemine, G., Nasser, W. & Reverchon, S. (1996). *Annu. Rev. Microbiol.* **50**, 213–257.
Jancarik, J. & Kim, S.-H. (1991). *J. Appl. Cryst.* **24**, 409–411.
Jenkins, J., Mayans, O. & Pickersgill, R. (1998). *J. Struct. Biol.* **122**, 236–246.
Khammas, K. M., Ageron, E., Grimont, P. A. D. & Kaiser, P. (1989). *Res. Microbiol.* **140**, 679–693.
La Fortelle, E. de & Bricogne, G. (1997). *Methods Enzymol.* **276**, 472–494.
Mateos, P. F., Jimenez-Zurdo, J. I., Chen, J., Squartini, A. S., Haack, S. K., Materínez-Molina, E., Hubbell, D. H. & Dazzo, F. B. (1992). *Appl. Environ. Microbiol.* **58**, 1816–1822.
Matthews, B. W. (1968). *J. Mol. Biol.* **33**, 491–497.
Otwinowski, Z. & Minor, W. (1997). *Methods Enzymol.* **276**, 307–326.
Pickersgill, R., Harris, G. & Jenkins, J. (1994). *Nature Struct. Biol.* **1**, 717–723.
Pissavin, C., Robert-Baudouy, J. & Hugouvieux-Cotte-Pattat, N. (1996). *J. Bacteriol.* **178**, 7187–7196.
Sawada, K., Ogawa, A., Ozawa, T., Sumitomo, N., Hatada, Y., Kobazyashi, T. & Ito, S. (2000). *Eur. J. Biochem.* **267**, 1510–1515.
Shevchik, V. E. & Hugouvieux-Cotte-Pattat, N. (1997). *Mol. Microbiol.* **24**, 1285–1301.
Shevchik, V. E., Robert-Baudouy, J. & Hugouvieux-Cotte-Pattat, N. (1997). *J. Bacteriol.* **179**, 7321–7330.